1A.5

Precipitation Analysis of Passive Microwave Data from the Advanced Microwave Precipitation Radiometer during the Tropical Cloud Systems and Processes Experiment

Frank J. LaFontaine*
Raytheon Information Solutions / NSSTC, Huntsville, Alabama

Daniel J. Cecil
University of Alabama – Huntsville / NSSTC, Huntsville, Alabama

Robbie E. Hood
NASA Marshall Space Flight Center / NSSTC, Huntsville, Alabama

1. INTRODUCTION

The Advanced Microwave Precipitation Radiometer (AMPR) is a passive microwave scanning radiometer which flew on the NASA ER-2 during the field-phase of the Tropical Cloud Systems Processes (TCSP) experiment conducted in July 2005. TCSP is collaboration between NASA, NOAA-HRD, universities, and the Costa Rican Weather Service to study tropical cyclogenesis and intensification.

AMPR produces calibrated brightness temperatures (Tb) at 10.7, 19.35, 37.1, and 85.5 GHz, ideal for studying precipitation (Spencer, et al., 1994). This paper will focus on the precipitation fields from AMPR as flown onboard the ER-2 during TCSP. An overview of category four Hurricane Emily on 17 July, development and landfall of Tropical Storm Gert from 23-25 July, and the development and intensification of Dennis from a weak tropical storm (05 July), to category one hurricane (06 July). Dennis was investigated again on 09 July as a category 1-2 hurricane, near the early stages of rapid intensification to category four. Finally, an overview of the AMPR Precipitation Index (API) for tropical systems from TCSP, and the Third and Fourth Convection and Moisture Experiments (CAMEX-3 1998 and CAMEX-4 2001) will be introduced.

Due to unresolved calibration issues remaining at the time of manuscript submission, the following discussion of the API for TCSP must be considered preliminary. The final calibration of the AMPR brightness temperatures for TCSP is in progress.

* *Corresponding author address:*
Frank J. LaFontaine, Raytheon / NSSTC,
320 Sparkman Dr., Huntsville, AL 35805
E-mail: frank.lafontaine@nsstc.nasa.gov.

2. AMPR PRECIPITATION INDEX

The AMPR Precipitation Index (API) gives a qualitative measure of rain intensity and precipitation ice content using the four AMPR frequencies (Hood, et al., 2006). The API is composed of a total 18 indices, two of which are non-precipitating cloud, along with a no cloud indicator. There are 6 potential rain levels within 4 potential ice levels. Of these 24 possible combinations, 8 have been rarely or never sampled to date. This leaves 16 precipitation indices within the API (Table 1).

The four ice levels indicate whether or not scattering is observed in three highest AMPR frequencies. When scattering is observed in a lower frequency (e.g., scattering at 37 GHz in addition to 85 GHz), that indicates the presence of larger ice particles (scattering a longer wavelength). It generally requires stronger updrafts to generate these larger graupel or hail particles. A combination of large and small ice particles along with supercooled liquid water (generally requiring strong updrafts) are the ingredients for substantial electric charge separation (Takahashi 1978). Therefore it is not surprising that we find enhanced electric fields with our higher ice levels.

When there is little or no appreciable ice (no 85 GHz ice-scattering signal) the rain intensity is limited to just the lower 3 levels (API 3-5) and electric field activity is insignificant. If only 85 GHz exhibits scattering (e.g., small graupel) then electric fields are weak (50 – 100 Vm-2).

API	Description	Criteria	Electric Field
0	*Clear*	*TB10<160 and TB37<215*	*none*
1	Moderate Cloud	TB19>190 or TB85>260	none
2	Heavy Cloud	TB85>270	none
	Ice Level 0	*TB85 ≥ TB37 or TB85 ≥ 275*	*< 50 Vm-2*
3	Rain Level 1	TB10>160 or TB37>215	insignificant
4	Rain Level 2	TB10>175	insignificant
5	Rain Levels 3-6	TB10>200	insignificant
	Ice Level 1	*TB85 < TB37 and TB85 < 275*	*< 100 Vm-2*
6	Rain Level 1	TB10>160 or TB37>215	weak
7	Rain Level 2	TB10>175	weak
8	Rain Level 3	TB10>200	weak
9	Rain Level 4	TB10>225	weak
10	Rain Levels 5-6	TB10>250	weak
	Ice Level 2	*TB37 < TB19 and Ice Level 1*	*< 1000 Vm-2*
11	Rain Level 1	TB10>160 or TB37>215	significant
12	Rain Level 2	TB10>175	significant
13	Rain Level 3	TB10>200	significant
14	Rain Level 4	TB10>225	significant
15	Rain Levels 5-6	TB10>250	significant
	Ice Level 3	*TB19 < TB10 and Ice Level 2*	*> 1000 Vm-2*
16	Rain Levels 1-4	TB10>160 or TB37>215	strong
17	Rain Level 5	TB10>250	strong
18	Rain Level 6	TB10>275	strong

Table 1: The description of the AMPR Precipitation Index and the relationship to electric fields.

If 37 GHz also indicates ice-scattering (e.g., large graupel, hail) now there are significant electric fields (100 – 1000 Vm-2). When 19 GHz is being scattered (large hail, etc.) then the lower 3 rain levels rarely occur but are included in rain level 4 (API 18). Here, the highest rain levels are observed and the electric fields are strong (> 1000 Vm-2).

The API is used to examine three major tropical systems sampled during TCSP. Note for all graphics of API, ice level 0 is in blue shades, ice level 1 is in green shades, ice level 2 is in yellow and red shades, and ice level 3 in purple shades. Refer to the URL http://tcsp.nsstc.nasa.gov/tcsp/ for GOES-11 movies of these storms.

3. SELECTED TCSP MISSIONS

Three missions of Dennis were flown, on 05, 06, and 09 July. These dates covered the development of Dennis from a tropical storm to a category three hurricane (Halverson, et al., 2006). In the 05 July mission (Figure 1), there is curvature in a widespread area of substantial ice and precipitation. The largest ice (API 16-18) was not indicated during this flight. At 0057 UTC on 07 July the eye of category one Dennis was forming with heavy precipitation and large ice in the southern eye wall (Figure 2). The third of four overpasses by the ER-2 of category 1-2 Dennis is shown in Figure 3, after Dennis had crossed Cuba. Note the eye of the hurricane has a large ice signature on the eastern quadrant. Cyclone precipitation banding is strongly indicated to the east, straddling 83W.

The lone mission to collect data from Hurricane Emily was on 17 July. By early that morning Emily has reached an impressive category 4 status. The ER-2 made two direct overpasses of the eye. In the second overpass shown in Figure 4, the API in the eye wall region is dominated by the highest indices. A well defined hurricane is clearly evident. Large hail and/or graupel surround at least half the eye wall

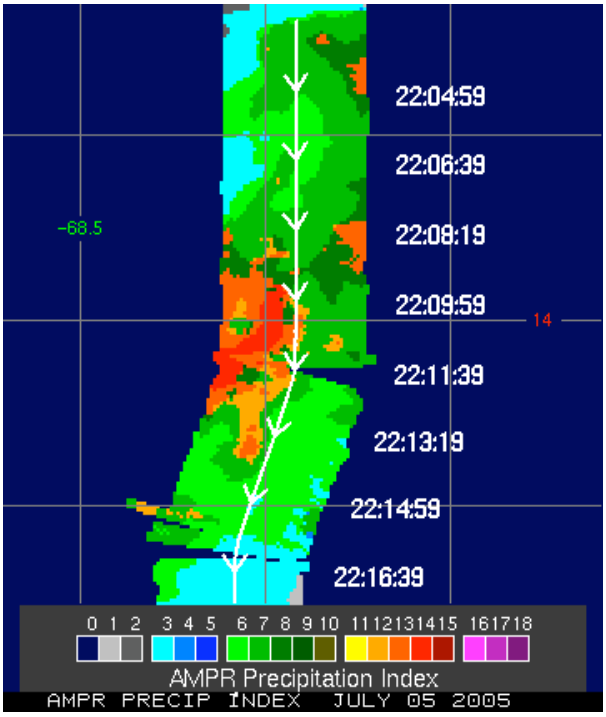

Figure 1: The API is displayed for tropical storm Dennis on 05 July 2005. Note the lack of ice level 3 (i.e., API 16-18), but a widespread area of substantial ice and precipitation.

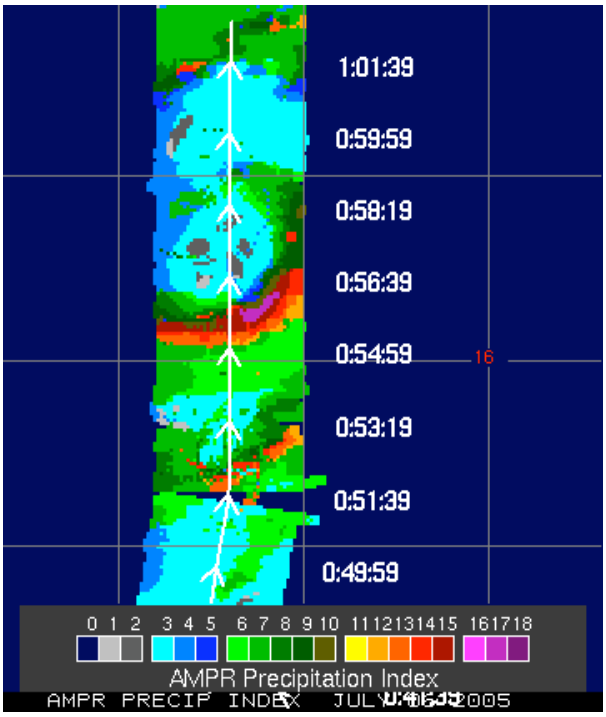

Figure 2: The API is displayed for category one Hurricane Dennis on 07 July 2005. Here, ice level 3 is beginning to appear and strong convection is evident in the band south of the center.

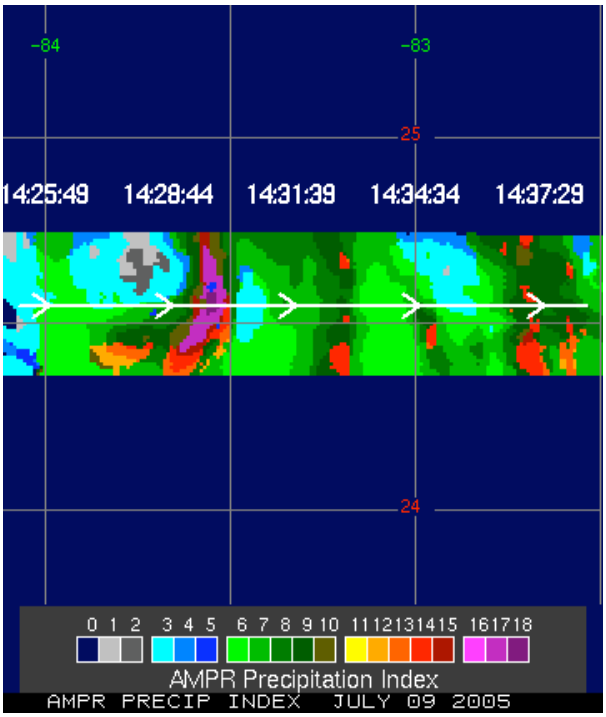

Figure 3: The API is displayed for tropical storm Dennis on 09July 2005. The anomalous 'blue' (index 5) result in the eye wall is due to an erroneous set of data points.

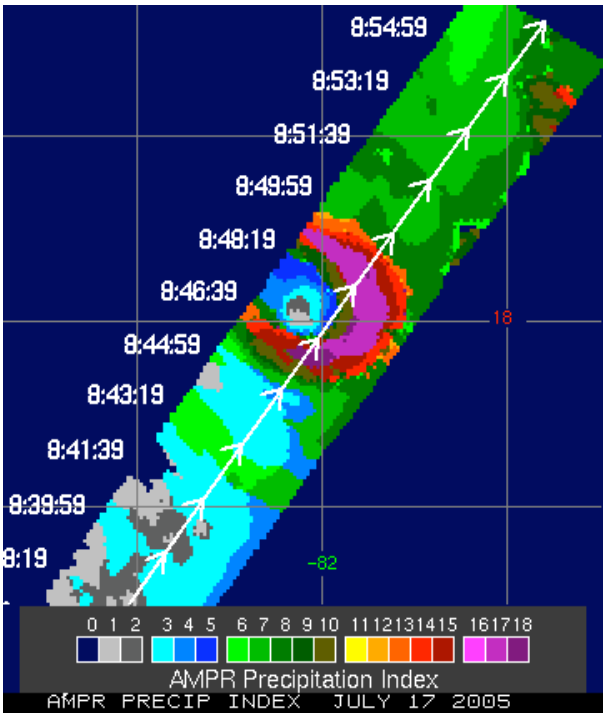

Figure 4: The API is displayed for Category 4 Hurricane Emily on 18 July2005.

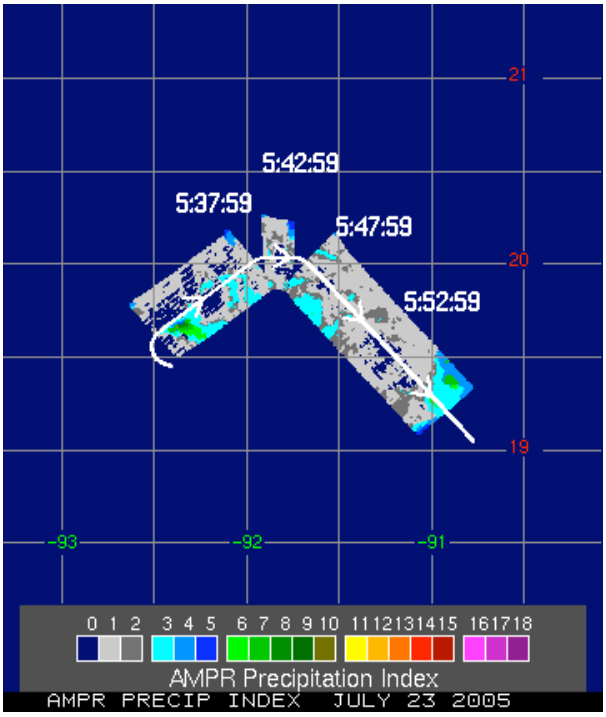

Figure 5: The API is displayed in the general area of the genesis of what will become Tropical Storm Gert (23 July 2005).

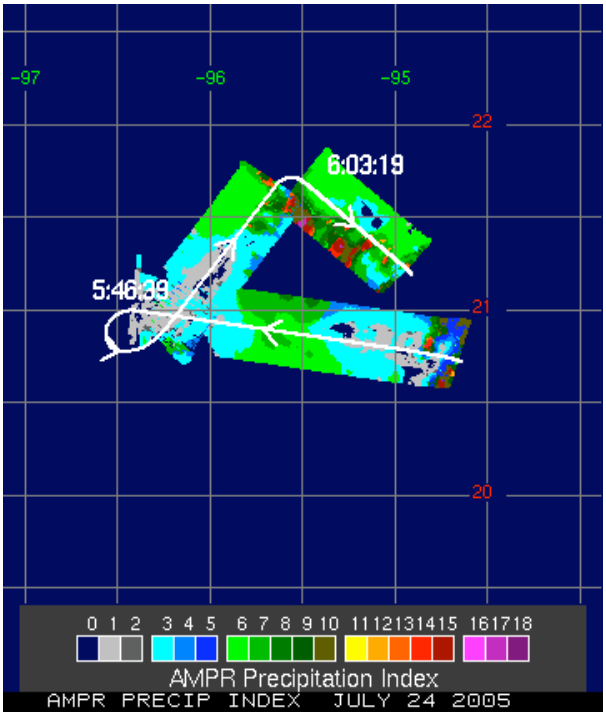

Figure 6: The API is displayed in an area of Tropical Depression Gert on 24 July 2005. Intense flare-ups of apparently deep convection are shown around 0603 UTC.

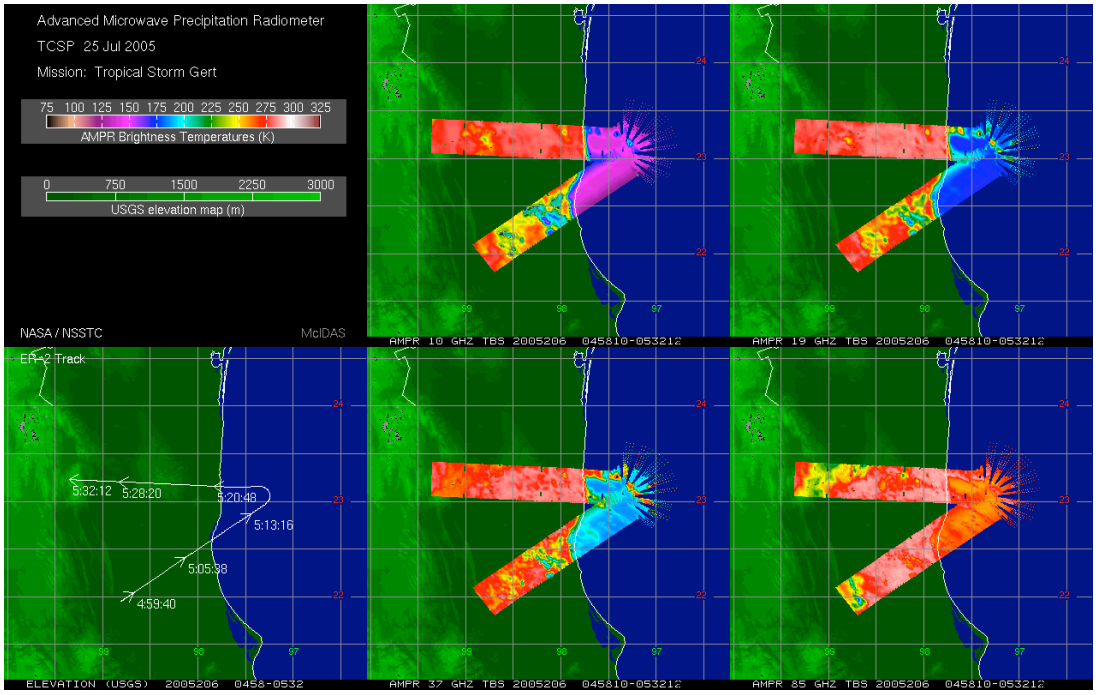

Figure 7: AMPR Tb are shown after landfall of Tropical Storm Gert on the eastern Mexico coast. Note, the API is an ocean-only product and not applicable in this context.

encompassing a large horizontal area (0.5 degree grid spacing). High amounts of precipitation spread to the NE of the core. The SW sector of this major hurricane has much less ice and rain at this time.

Three missions of Gert were flown on consecutive days (23-25 July). The storm was just an open wave near the Yucatan Peninsula on 23 July, becoming a tropical storm on 24 July, and made landfall in eastern Mexico just prior to the 25 July mission. The API indices are greatest in the developing convection throughout the period (Figure 5 in green and Figure 6 in red). Since the API is an ocean-only product, the landfall of Gert on 25 July is shown as Tb imagery in Figure 7. Large amounts of inland surface water can be seen at 10 GHz (blue shades). The higher elevations in red and white at 10 GHz indicate relatively little surface water.

4. ANALYSIS

This general overview of the TCSP missions suggests that the preliminary API show the largest ice mass and rainfall in the stronger systems as expected. Areas where API is highest also correspond to the highest electric fields (not shown).

To further the investigation, the AMPR TCSP data set was combined with data from other AMPR missions targeted at tropical cyclones and cyclogenesis. This comprises the largest collection of passive microwave data from aircraft targeted directly at these types of systems known to date.

In this study, data have been merged with the data from two previous experiments where tropical systems were also heavily sampled, CAMEX-3 and CAMEX-4. A statistical analysis was performed using all the available API data. It is recognized, for one, that biases may be large in analyses of this type due to incomplete and non-uniform coverage of the large systems from the current aircraft platform.

There have been 21 ER-2 missions since 1998 where AMPR collected tropical cyclone data. The storms have been grouped into 6 categories, 4 missions of which are not used in this study (see Table 2). Figures 8 and 9 illustrate the percentage of each ice and rain level per storm category respectively. The percentage is relative to the sum of all precipitating pixels (i.e., APIs 3-18) per level. The following bullets point to some of the trends observed from the two plots:

- major hurricanes and strengthening systems are analogous in ice level and rain level distribution.
- weakening systems have relatively little occurrence of high ice levels (2-3).
- category 1-2 steady-state hurricanes show resemblance to weakening systems but still have more ice scattering in comparison.
- weakening systems have the greatest percentage of light rain rates and least amount of high rain rates, which may be an important indicator of dissipation.

Note, the relative nature of the percentage magnitudes (e.g., ~95% ice levels 0-1, < 5% ice levels 2-3; rain levels analogously) is a natural occurrence in the majority of tropical systems, where large regions of precipitation are primarily stratiform or weak convection (Cecil, et al., 2002).

5. DISCUSSION

This may suggest that major hurricanes and strengthening tropical systems of any type exhibit similar hydrometeor characteristics. Large amounts of ice mass are maintained and/or generated compared to the weaker systems. Rainfall is enhanced.

The strongest ice scattering (level 3) and heaviest rain rates (level 6) are observed 2-3 time more often in the major hurricanes or strengthening systems than in the weaker hurricanes and weakening systems. The significant ice scattering associated with high API suggests vigorous vertical updrafts in these areas.

This is consistent with previous studies, in which increased areal coverage of significant ice scattering is associated with storms that are either intensifying or already intense (Cecil and Zipser, 1999).

The authors are grateful to Dr. Ramesh Kakar, the NASA Weather Focus Area Lead, who funded this effort. Also, thanks to the AMPR engineering staff, the ER-2 pilots and crew, and the TCSP project office who contributed to or facilitated the data collection necessary for this work.

Storm Category	Storm Name	Mission Date	Experiment	Pre-Mission			Post-Mission		
				Cat	knots	mb	Cat	knots	mb
Steady-State Major Hurricanes	Bonnie	23 Aug 1998	CAMEX-3	3	100	958	3	100	954
	Bonnie	24 Aug 1998	CAMEX-3	3	100	962	3	100	962
	Bonnie	26 Aug 1998	CAMEX-3	3	100	964	3	100	962
	Emily	17 Jul 2005	TCSP	4	135	929	4	130	946
Steady-State Hurricanes	Danielle	30 Aug 1998	CAMEX-3	1	65	990	1	70	983
	Georges	21 Sep 1998	CAMEX-3	2	95	966	2	90	970
	Georges	25 Sep 1998	CAMEX-3	2	90	982	2	90	974
	Georges	27 Sep 1998	CAMEX-3	2	95	962	2	95	961
	Humberto	23 Sep 2001	CAMEX-4	1	80	986	1	75	989
	Humberto	24 Sep 2001	CAMEX-4	1	70	991	1	65	992
Steady-State Non-Hurricanes	Gert	23 Jul 2005	TCSP	PG	n/a	n/a	PG	n/a	n/a
	Gert	24 Jul 2005	TCSP	TD	30	1009	TS	35	1008
Strengthening Systems	Gabrielle	16 Sep 2001	CAMEX-4	TS	55	995	1	65	991
	Humberto	22 Sep 2001	CAMEX-4	TS	40	1007	TS	55	995
	Dennis	05 Jul 2005	TCSP	TS	35	1007	TS	45	1000
	Dennis	06 Jul 2005	TCSP	TS	60	989	1	80	972
	Dennis	09 Jul 2005	TCSP	1	75	973	2	90	962
Weakening Systems	Earl	02 Sep 1998	CAMEX-3	2	85	988	1	70	987
	Erin	10 Sep 2001	CAMEX-4	3	100	969	1	80	973
Landfalling Systems	Georges	22 Sep 1998	CAMEX-3	2	95	970	1	65	990
	Gert	25 Jul 2005	TCSP	TS	40	1005	TD	25	1006

Table 2: Shown are the AMPR data sets available for the API analysis. The categories "Landfalling Systems" and "Steady-State Non-Hurricanes" (gray shaded) are not used in this study. Note, PG means pre-genesis. The meteorological data are from the NHC best track for all except Emily, which uses operational estimates from the Weather Underground web-site. The time difference in the pre- to post-mission track information is 12 hours for all missions.

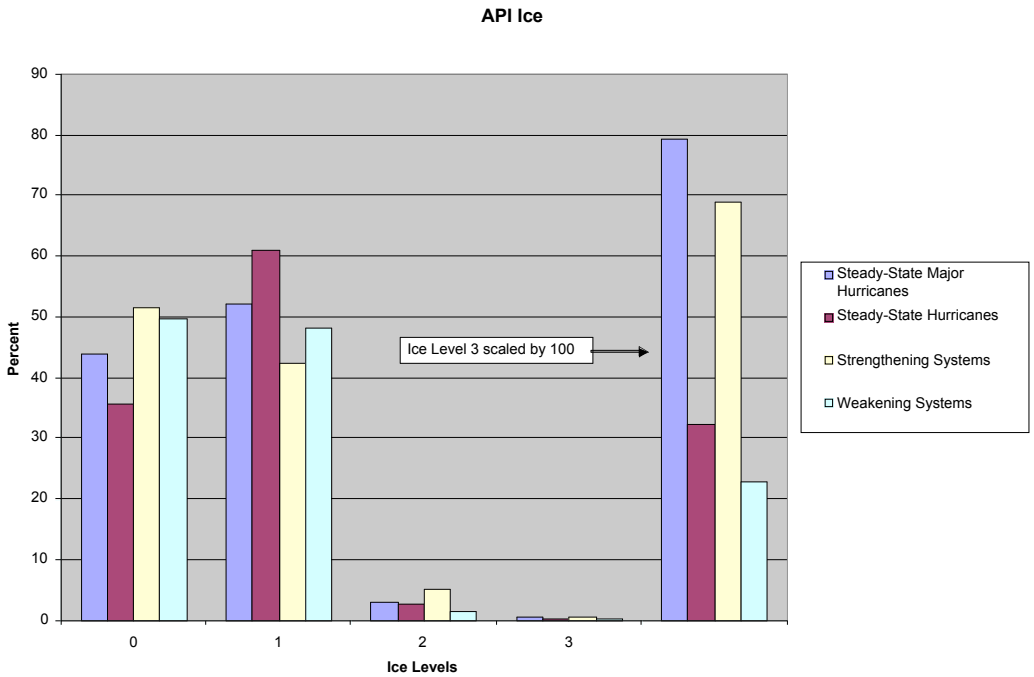

Figure 8: Shown are the API ice levels for each of the storm categories. Ice level 0 indicates little or no appreciable ice, ice level 1 includes small graupel, ice level 2, graupel and small hail, ice level 3, large graupel and hail. Ice level 3 is exaggerated to show detail.

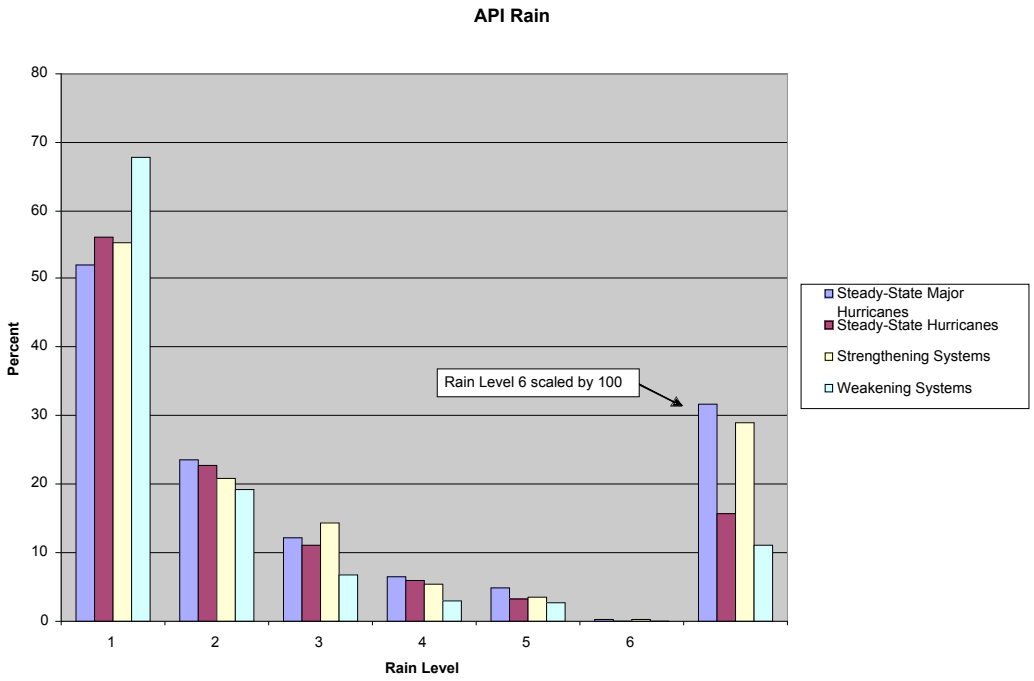

Figure 9: Shown are the API rain levels for each of the storm categories. Rain levels are linearly related to Tb. Rain level 6 is exaggerated to show detail.

5. REFERENCES

Cecil, D.J. and E.J. Zipser, 1999: Relationships between tropical cyclone intensity and satellite-based indicators of inner core convection: 85-GHz ice-scattering signature and lightning. *Mon. Wea. Rev*, **127**, 103-123.

Cecil, D.J., Zipser, E. J., and S. W. Nesbitt, 2002: Reflectivity, ice scattering, and lightning characteristics of hurricane eyewalls and rainbands. Part I: Quantitative description. *Mon. Wea. Rev*, **130**, 769-784.

Halverson J., P. L. Azofeifa, M. Black, S. Braun, D. Cecil, M. Goodman, A. Heymsfield, G. Heymsfield, R. Hood, T. Krishnamurti, G. McFarquhar, J. Molinari, R. Rogers, J. Turk, C. Velden, D.-L. Zhang, E. Zipser, and R. Kakar, 2006: NASA's Tropical Cloud Systems and Processes (TCSP) Experiment: Investigating Tropical Cyclogenesis and Hurricane Intensity Change. *Submitted to Bull. Amer. Meteor. Soc*.

Hood, R. E., D. J. Cecil, F. J. LaFontaine, R. J. Blakeslee, D. M. Mach, G. M. Heymsfield, F. D. Marks, Jr., E. J. Zipser, and H. M. Goodman, 2006: Classification of Tropical Oceanic Precipitation using High Altitude Aircraft Microwave and Electric Field Measurements. *J. Atmos. Sci.*, **63**, 218-233.

Spencer, R. W., R. E. Hood, F. J. LaFontaine, E. A. Smith, R. Platt, J. Galliano, V. L.. Griffin, and E. Lobl, 1994: High resolution imaging of rain systems with the Advanced Microwave Precipitation Radiometer. *J. Atmos. Oceanic Tech.*, **11**, 849-857.

Takahashi, T., 1978: Riming electrification as a charge generation mechanism in thunderstorms. *J. Atmos. Sci.*, **35**, 1536–1548.